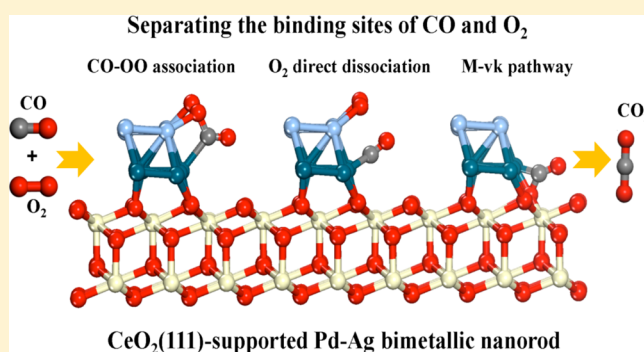


Computational Design of a CeO₂-Supported Pd-Based Bimetallic Nanorod for CO Oxidation

Bing Liu,[†] Zhen Zhao,^{*,†} Graeme Henkelman,^{*,‡} and Weiyu Song[†][†]State Key Laboratory of Heavy Oil Processing, College of Science, China University of Petroleum, Beijing, Beijing 102249, P. R. China[‡]Department of Chemistry and the Institute for Computational and Engineering Sciences, University of Texas at Austin, Austin, Texas 78712-0165, United States

Supporting Information

ABSTRACT: Engineering a bimetallic system with complementary chemical properties can be an effective way of tuning catalytic activity. In this work, CO oxidation on CeO₂(111)-supported Pd-based bimetallic nanorods was investigated using density functional theory calculations corrected by on-site Coulomb interactions. We studied a series of CeO₂(111)-supported Pd-based bimetallic nanorods (Pd–X, where X = Ag, Au, Cu, Pt, Rh, Ru) and found that Pd–Ag/CeO₂ and Pd–Cu/CeO₂ are the two systems where the binding sites of CO and O₂ are distinct; that is, in these two systems, CO and O₂ do not compete for the same binding sites. An analysis of the CO oxidation mechanisms suggests that the Pd–Ag/CeO₂ system is more effective for catalyzing CO oxidation as compared to Pd–Cu/CeO₂ because both CeO₂ lattice oxygen atoms and adsorbed oxygen molecules at Ag sites can oxidize CO with low energy barriers. Both the Pd–Ag and Pd–CeO₂ interfaces in Pd–Ag/CeO₂ were found to play important roles in CO oxidation. The Pd–Ag interface, which combines the different chemical nature of the two metals, not only separates the binding sites of CO and O₂ but also opens up active reaction pathways for CO oxidation. The strong metal–support interaction at the Pd–CeO₂ interface facilitates CO oxidation by the Mars–van Krevelen mechanism. Our study provides theoretical guidance for designing highly active metal/oxide catalysts for CO oxidation.



1. INTRODUCTION

Catalytic CO oxidation has been extensively studied not only because of its industrial importance but also as a prototypical reaction in heterogeneous catalysis.¹ Because of a remarkable oxygen storage capacity,^{2–4} ceria-based catalysts have been widely used for low-temperature CO oxidation.⁵ Recently, Pd-based catalysts, which have a high oxygen adsorption ability and a lower cost than Pt- and Rh-based catalysts,^{6–8} have attracted considerable attention, for example, as a replacement for the expensive catalysts used to remove CO from vehicle exhaust.⁸ Experimental studies have shown that ceria-supported Pd catalysts have a high activity for catalytic CO oxidation.^{9–11}

In our previous theoretical study,¹² we studied the reaction mechanism of CO oxidation on a CeO₂-supported Pd nanorod. A limitation of the CeO₂-supported Pd system for CO oxidation is that CO and O₂ need to compete for the same Pd binding sites. The high adsorption energy of CO to Pd can result in CO poisoning, which hinders the coadsorption of O₂ and thus prevents CO oxidation. It is therefore desirable to separate the binding sites of CO and O₂.

Bimetallic catalysts have been widely used in heterogeneous catalysis.¹³ Adding a second metal can be an effective strategy to tune catalytic performance through modification of

electronic and structural factors^{13,14} or via a bifunctional effect in which atoms of the two metals provide catalytic sites which play unique roles, such as separating the adsorption of different reactants or intermediates.¹⁵ Designing a CeO₂-supported Pd-based bimetallic system where the binding sites of CO and O₂ are separated is our goal for improving CO oxidation activity.

For oxide-supported metal catalysts, it has been recognized that the interface between the oxide support and the supported metal can have a pronounced effect on the catalytic activity.^{16–20} Green et al. reported that Au–TiO₂ interfacial sites are active for CO oxidation, partial oxidation of acetic acid, and low-temperature H₂ oxidation.¹⁶ Cargnello et al. also found that ceria–metal interfacial sites greatly enhance the activity of CO oxidation.¹⁸ The explicit role of interfacial sites has additional support from the clear relationship between the length of the Au–CeO₂ interface and the CO oxidation activity on Au–CeO₂ multilayers.¹⁹

The nature of metal–oxide interfacial effects has been the subject of considerable debate. Bruix et al. suggested that strong

Received: January 9, 2016

Revised: February 21, 2016

Published: February 24, 2016

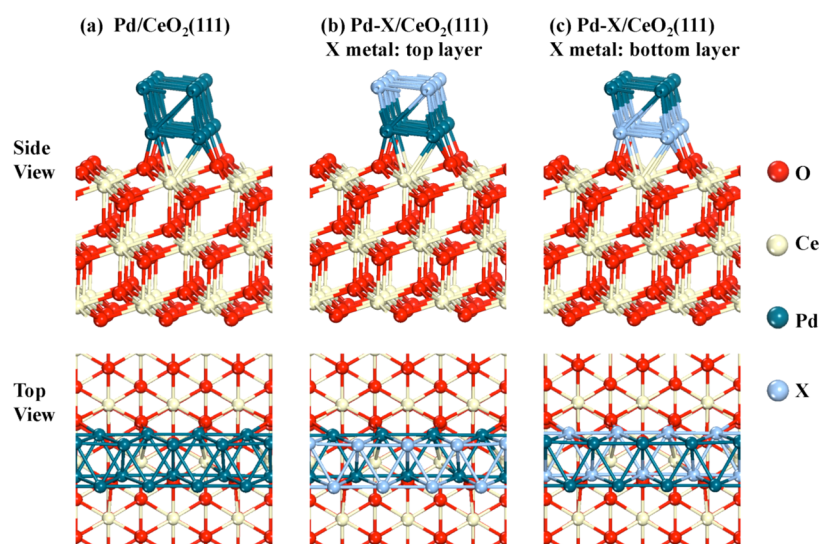


Figure 1. Structures of $\text{CeO}_2(111)$ -supported (a) Pd nanorod and (b, c) bimetallic Pd–X nanorods where the X metal is in the top and bottom layers, respectively.

electronic perturbations induced by Pt– CeO_2 interactions lead to the high catalytic activity at the interface of $\text{Pt}_8/\text{CeO}_2(111)$.²¹ Aranifard et al. proposed that the high activity for the water-gas shift reaction at the interface of Pt/ CeO_2 catalysts originates from the interfacial oxygen vacancies, which facilitate water activation and dissociation.²⁵ The formation of a thin Pd oxide layer at the Pd– Fe_3O_4 interface has also been proposed to be the origin of the high activity for CO oxidation on Pd/ Fe_3O_4 catalysts.²³ The origin of metal–support interfacial effects remain a controversial topic.

In this work, we carry out density functional theory calculations corrected by on-site Coulomb interactions (DFT+U) to investigate the reaction mechanisms of CO oxidation over Pd-based bimetallic nanorods supported on $\text{CeO}_2(111)$. We identify a $\text{CeO}_2(111)$ -supported Pd–Ag bimetallic system which separates the binding sites of CO and O_2 and provides active reaction pathways for CO oxidation with low energy barriers. Both the Pd–Ag and Pd– CeO_2 interfaces in this system are found to play important roles in CO oxidation.

2. COMPUTATIONAL DETAILS

2.1. Computational Methods. All the DFT calculations were performed using the Vienna *ab initio* simulation package (VASP).^{24,25} To accurately treat the highly localized Ce 4f-orbitals, we conducted spin-polarized DFT+U calculations with a value of $U_{\text{eff}} = 5.0$ eV applied to the Ce 4f states.²⁶ This U_{eff} value has been reported to describe the electronic structure of reduced ceria in previous studies.^{27,28} The projector-augmented wave method was used to represent core–valence interactions.²⁹ Valence electrons were described by a plane wave basis with an energy cutoff of 400 eV. The generalized gradient approximation with the Perdew–Burke–Ernzerhof functional was used to model electronic exchange and correlation.³⁰ Gaussian smearing with a width of 0.05 eV was used to improve convergence of states near the Fermi level. The Brillouin zone was sampled at the Gamma point. Optimized structures were obtained by minimizing the forces on each ion until they were less than 0.05 eV/Å.

The adsorption energy was defined as

$$E_{\text{ads}} = E(\text{adsorbate} + \text{surface}) - E(\text{adsorbate}) - E(\text{surface})$$

where $E(\text{adsorbate} + \text{surface})$ is the total energy of the adsorbate interacting with the surface; $E(\text{adsorbate})$ and $E(\text{surface})$ are the energies of the free adsorbate in gas phase and the bare surface, respectively. A negative value corresponds to exothermic adsorption, with more negative values corresponding to stronger binding.

Transition states (TSs) for the elementary reactions were located using the climbing-image nudged elastic band method^{31,32} and were confirmed as having a single imaginary frequency. Energy barriers (E_{bar}) were calculated as the energy difference between the transition and initial states.

2.2. Computational Models. It has been demonstrated that the $\text{CeO}_2(111)$ surface is the most stable among the three low index surfaces of ceria, namely $\text{CeO}_2(111)$, (110), and (100).^{33,34} Accordingly, a slab model of $\text{CeO}_2(111)$ surface was used in this work, consisting of 9 atomic layers (three trilayers) with a 3×3 surface supercell. The CeO_2 slab contains 81 atoms and is separated from periodic images by a 12 Å vacuum gap perpendicular to the surface. During geometry optimization, the atoms in the bottom three atomic layers were fixed at their bulk-truncated positions; all other atoms were allowed to relax. The CeO_2 -supported Pd nanorod system was modeled by adding a two-layer Pd rod on the top of the stoichiometric $\text{CeO}_2(111)$ surface, as shown in Figure 1a, which has been described in our previous work.¹² The Pd–X bimetallic nanorod (where X is Ag, Au, Cu, Pt, Rh, or Ru) was modeled by replacing one Pd layer with a X metal layer, as shown in Figures 1b and 1c.

In order to determine whether the X metal layer prefers to be in the top layer or bottom layer, the exchange energy E_{ex} is calculated, defined as the energy change due to exchange of the top X metal layer with the bottom Pd layer

$$E_{\text{ex}} = E_{\text{X-bottom}} - E_{\text{X-top}}$$

A negative E_{ex} value indicates that the X metal layer prefers to be in bottom layer. Table 1 contains the calculated exchange energies E_{ex} for the bimetallic Pd–X/ CeO_2 systems. These results indicate that Ag and Au prefer to be in the top layer, as shown in Figure 1b. Cu, Pt, Rh, and Ru prefer to be in the bottom layer, as shown in Figure 1c.

Table 1. Calculated Exchange Energy E_{ex} for the Bimetallic Pd–X/CeO₂ Systems

alloying element X	Ag	Au	Cu	Pt	Rh	Ru
E_{ex} (eV)	1.01	1.69	–2.45	–0.31	–2.91	–6.46

3. RESULTS

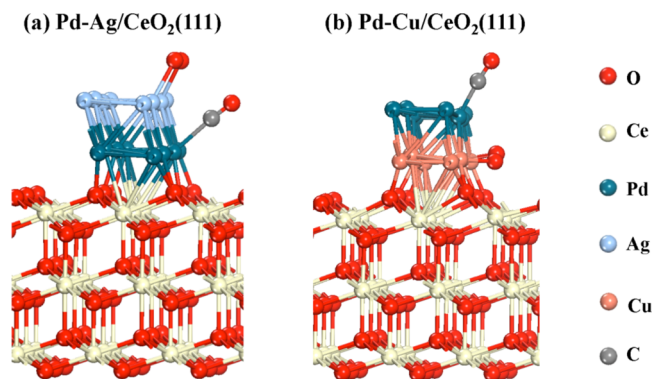
3.1. Separating the Binding Sites of CO and O₂. The binding energies of CO and O₂ on the Pd and X-metal layers of the six bimetallic Pd–X/CeO₂ systems were calculated, as shown in Table 2. It can be seen that CO binds more strongly than O₂ at all of the binding sites in the Pd–Au, Pd–Pt, Pd–Rh, and Pd–Ru systems, indicating that they would become saturated by CO under CO oxidation conditions.

In the case of the Pd–Ag system, the Pd layer prefers CO binding while Ag prefers O₂ binding; the two reactants have distinct binding sites. In the case of the Pd–Cu system, the Pd layer also binds CO (–1.71 eV) more strongly than O₂ (–1.02 eV) while the Cu layer prefers to bind O₂. Therefore, Pd–Ag and Pd–Cu are the two systems which separate the binding sites of CO and O₂. The adsorption geometry of CO and O₂ on the Pd–Ag/CeO₂ and Pd–Cu/CeO₂ systems are shown in Figure 2. These two systems were selected for analysis of CO oxidation mechanism.

3.2. CO Oxidation on CeO₂-Supported Pd–Ag Bimetallic System. Three reaction pathways for CO oxidation on Pd–Ag/CeO₂ were considered, including the (1) CO–OO association pathway, (2) direct O₂ dissociation pathway, and (3) Mars–van Krevelen mechanism.

3.2.1. CO–OO Association Pathway. The calculated structures of the intermediates and transition states in the CO–OO association reaction pathway and the corresponding energy profile are shown in Figure 3. First, O₂ binds to the Ag layer (IM1 in Figure 3) and CO binds to the Pd layer (IM2). These two molecules react with a energy barrier of 0.45 eV (TS1) to form an OCOO intermediate (IM3). CO₂ is released from the OCOO intermediate by breaking the O–O bond in a spontaneous and exothermic process (IM4). A desorption energy of 0.21 eV is required for CO₂ desorption (IM5). Then, a second CO molecule adsorbs on the Pd layer (IM6) to react with the remaining atomic O at the Pd–Ag interface with an energy barrier of 0.42 eV (TS2), leading to the formation of an adsorbed CO₂ molecule (IM7). Finally, CO₂ desorbs into the gas phase (FS), closing the catalytic cycle.

3.2.2. Direct O₂ Dissociation Pathway. In the direct O₂ dissociation pathway, as shown in Figure 4, the adsorbed O₂ on the Ag layer dissociates into two oxygen atoms (IM2) with a low energy barrier of 0.31 eV (TS1). This O₂ dissociation process is exothermic by 1.29 eV. Next, CO adsorbs on the Pd site (IM3) and reacts with a dissociated O atom to form an adsorbed CO₂ complex (IM4) with a very low energy barrier of 0.04 eV (TS2). This energy barrier is much lower than that for CO oxidation by the coadsorbed O₂ in the CO–OO

**Figure 2.** Calculated structures of CO and O₂ adsorption on the Pd–Ag/CeO₂ and Pd–Cu/CeO₂ systems.

association pathway discussed previously. An energy of 0.19 eV is then required for CO₂ desorption (IM5). Next, a second CO molecule adsorbs on the Pd layer (IM6) and reacts with the other dissociated O atom to form CO₂ (IM7) with an energy barrier of 0.42 eV (TS3).

3.2.3. Mars–van Krevelen Mechanism: CO Oxidation by Lattice Oxygen at Interface. The Mars–van Krevelen (M–vK) process, as shown in Figure 5, starts with a reaction between an adsorbed CO molecule on the Pd layer and a lattice O atom of CeO₂(111) at the Pd–CeO₂ interface. A CO molecule adsorbs on Pd site (IM1 in Figure 5) and reacts with an adjacent lattice oxygen atom to form a triangular type CO₂ intermediate (IM2; 0.57 eV barrier through TS1). The desorption of CO₂ leaves an oxygen vacancy on the CeO₂(111) surface (IM3). A gas-phase O₂ molecule then spontaneously adsorbs at this vacancy (IM4) and a second CO molecule adsorbs on the Pd layer (IM5) to react with the adsorbed O₂ species forming adsorbed CO₂ (IM6; 0.46 eV barrier through TS2). Finally, CO₂ desorbs into the gas phase (FS) and the oxygen vacancy of CeO₂(111) is filled by the remaining O atom to complete the catalytic cycle.

3.3. CO Oxidation on CeO₂-Supported Pd–Cu Bimetallic System. Three reaction pathways for CO oxidation on Pd–Cu/CeO₂ system were also considered, including the (1) CO–OO association, (2) direct O₂ dissociation, and (3) oxygen spillover.

3.3.1. CO–OO Association Pathway. Following the reaction pathway in Figure 6, O₂ binds to the Cu layer (IM1) and CO binds to the Pd layer (IM2). These two molecules react with an energy barrier of 0.35 eV (TS1) to form an OCOO intermediate (IM3). The formation of CO₂ from OCOO is spontaneous and exothermic by 1.95 eV (IM4). CO₂ desorption requires an energy of 0.48 eV (IM5). Next, a second CO molecule adsorbs (IM6) and reacts with the remaining atomic O to form CO₂ (IM7; 0.47 eV barrier through TS2) which then spontaneously desorbs into the gas phase (FS).

Table 2. Binding Energies of CO and O₂ on All the Bimetallic Pd–X/CeO₂ Systems

		binding energy, (eV)					
		Pd–Ag	Pd–Au	Pd–Cu	Pd–Pt	Pd–Rh	Pd–Ru
Pd layer	CO	–1.66	–1.10	–1.71	–1.47	–1.50	–1.84
	O ₂	–1.10	–0.98	–1.02	–1.16	–1.29	–1.33
alloying metal layer	CO	–0.52	–0.69		–1.94	–1.92	–2.16
	O ₂	–0.54	–0.31	–1.00	–0.78	–1.52	–1.57

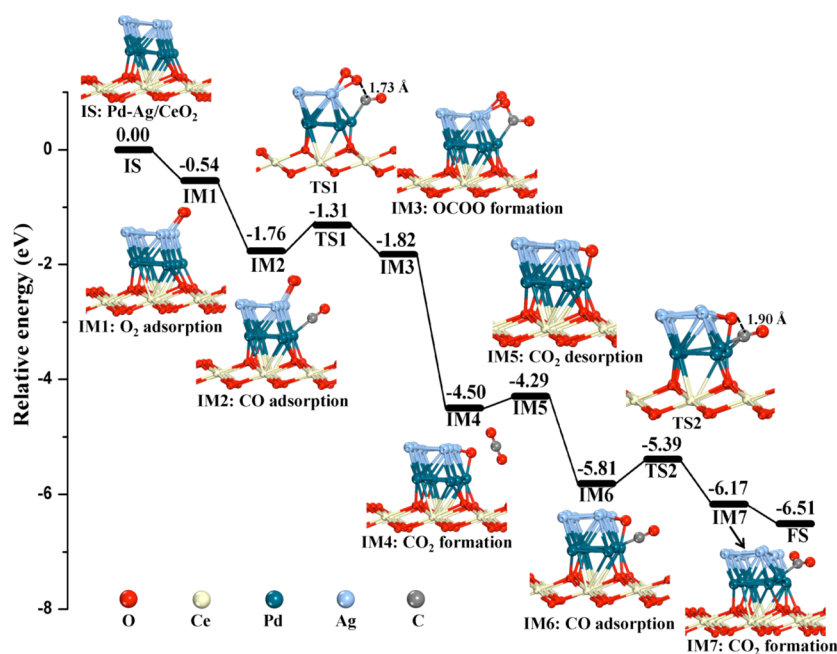


Figure 3. Calculated structures and energy profile in the CO–OO association pathway on Pd–Ag/CeO₂(111).

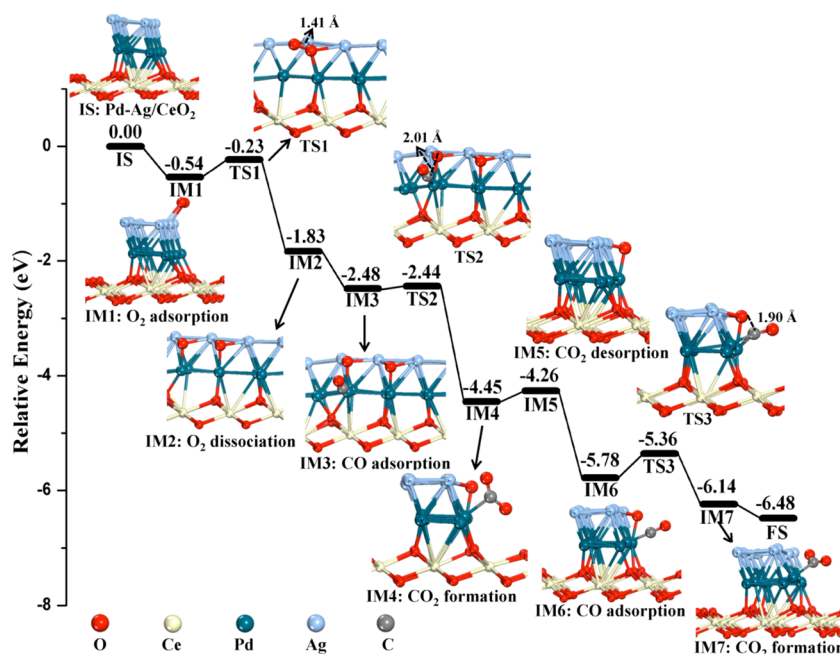


Figure 4. Calculated structures and energy profile in the direct O₂ dissociation pathway on Pd–Ag/CeO₂(111).

3.3.2. Direct O₂ Dissociation Pathway. In the direct O₂ dissociation pathway, as shown in Figure 7, O₂ adsorbs on the Cu layer and dissociates into two oxygen atoms (IM2) with an energy barrier of 0.55 eV (TS1). CO then adsorbs on the Pd site (IM3) and reacts with a dissociated O atom to form an adsorbed CO₂ complex (IM4). This CO oxidation process has a high energy barrier of 1.86 eV (TS2), which is much higher than that for CO oxidation by coadsorbed O₂ in the CO–OO association pathway discussed previously. This high energy barrier can be attributed to the stability of the O atom at the Cu site. Palagin et al. studied the Pd₄Cu₂ cluster and proposed that the higher affinity of oxygen for Cu eventually leads to the poisoning of the catalyst.³⁵ Zhang et al. studied the CO

oxidation on Au–Cu bimetallic nanocluster and proposed that oxygen atoms can oxidize the Cu atoms, converting them to Cu₂O or CuO₂ and thus deactivating the active sites.³⁶ An energy of 0.24 eV is then required for CO₂ desorption (IM5). Subsequently, a second CO molecule adsorbs on the Pd layer (IM6) and reacts with the other dissociated O atom, crossing a barrier of 0.47 eV (TS3) forming CO₂ (IM7) which readily desorbs.

3.3.3. Oxygen Spillover Mechanism. In the Pd–Cu system, CO binds to the top Pd layer and O₂ binds to the bottom Cu layer, so that CO cannot directly interact with the lattice oxygen atom at the Cu–CeO₂ interface. Alternatively, Vayssilov et al. proposed that oxygen spillover from nanostructured CeO₂

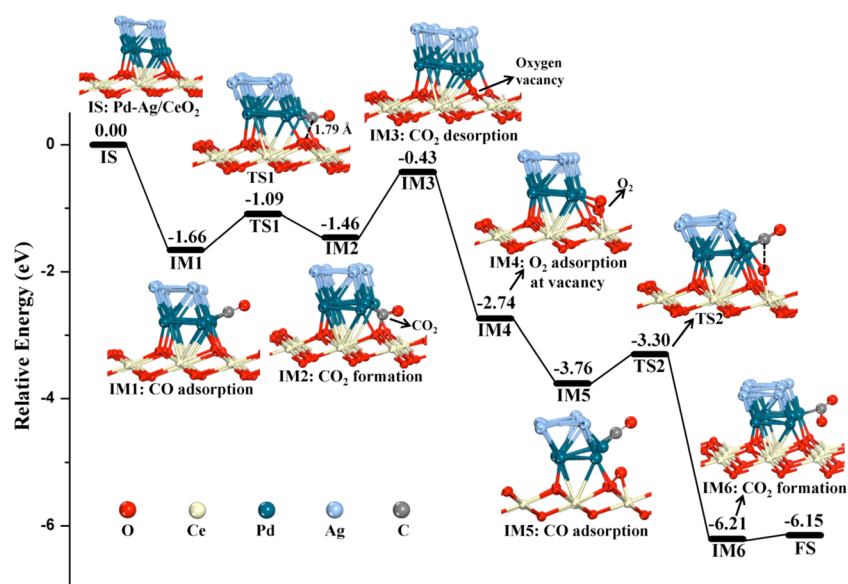


Figure 5. Calculated structures and energy profile in the M–vK mechanism on Pd–Ag/CeO₂(111).

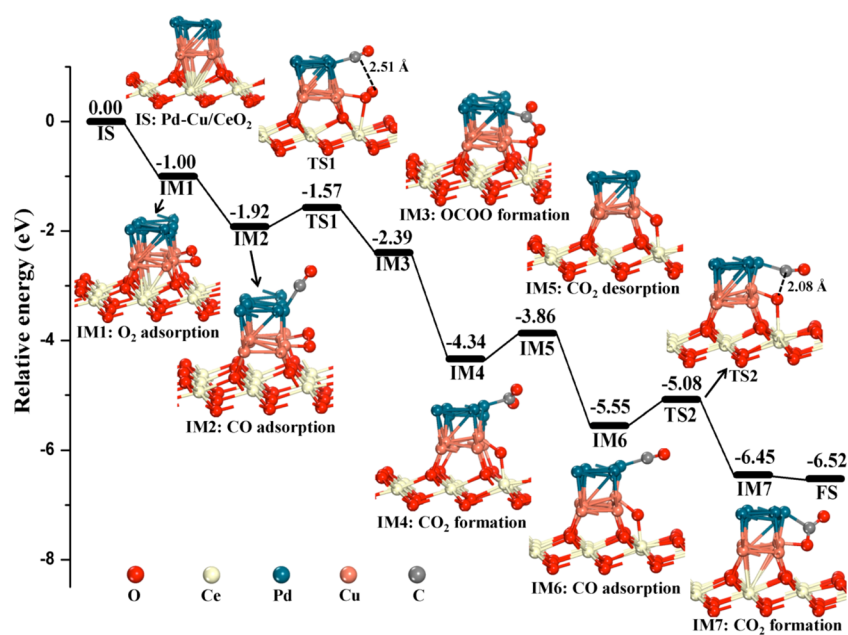


Figure 6. Calculated structures and energy profile in the CO–OO association pathway on Pd–Cu/CeO₂(111).

to the supported Pt nanoparticles occurs, and the transferred oxygen acts as the active species for CO oxidation.³⁷ In order to determine whether lattice oxygen atoms in CeO₂ can take part in CO oxidation, we calculated the energetics of lattice oxygen spillover from the CeO₂(111) surface to the Cu layer. We find that the oxygen spillover in our case is endothermic by 1.32 eV (as shown in Figure 8), indicating that this process is energetically prohibited. This is consistent with a report by Kim et al. that oxygen spillover is energetically unfavorable for Au clusters supported on CeO₂(111).³⁸ Therefore, in the Pd–Cu/CeO₂(111) system, the lattice oxygen atoms in CeO₂(111) cannot react with the adsorbed CO on the top Pd layer.

4. DISCUSSION

4.1. Comparison between Pd–Ag System and Pd–Cu System. The Pd–Ag/CeO₂ and Pd–Cu/CeO₂ systems both

separate the binding sites of CO and O₂, but they have different structures and correspondingly different reaction mechanisms and catalytic activity. For Pd–Ag/CeO₂, the CeO₂ support binds to the Pd layer, while for Pd–Cu/CeO₂, the CeO₂ support binds to the Cu layer. The CeO₂ lattice oxygen in Pd–Ag/CeO₂ can react with adsorbed CO at the Pd–CeO₂ interface. In contrast, in the Pd–Cu/CeO₂ system, the CeO₂ lattice oxygen atoms cannot react with adsorbed CO. Therefore, Pd–Ag/CeO₂ is expected to be better for CO oxidation because both CeO₂ lattice oxygen atoms and adsorbed oxygen molecules can oxidize CO, both with a low energy barrier.

The dominant reaction pathway for CO oxidation is also different in these two systems. The direct O₂ dissociation pathway is dominant for CO oxidation on Pd–Ag/CeO₂ due to the low energy barriers, while the CO–OO association pathway

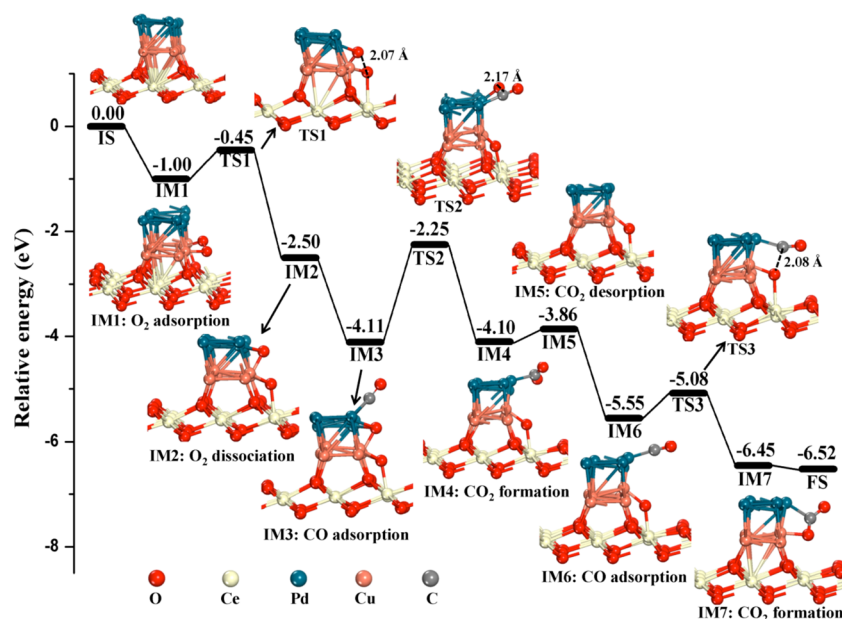


Figure 7. Calculated structures and energy profile in the direct O_2 dissociation pathway on Pd–Cu/CeO₂(111).

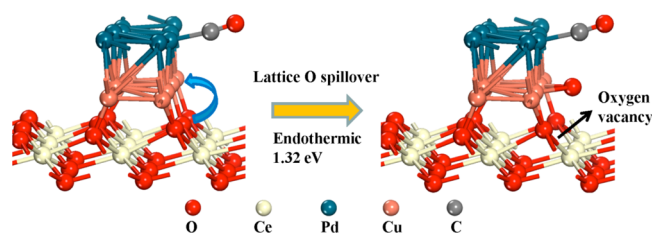


Figure 8. Lattice oxygen spillover from the CeO₂(111) surface to the Cu layer.

is favorable for CO oxidation on Pd–Cu/CeO₂. The affinity of oxygen for the Cu layer in the Pd–Cu/CeO₂ system leads to a high stability of the O atom at the Cu layer, energetically preventing the oxidation of CO.

4.2. Comparison with CO Oxidation on CeO₂-Supported Pd Monometallic System. Compared with the CeO₂-supported Pd monometallic system in our previous study,¹² on the one hand, the Pd–Ag bimetallic system can generate a potential oxygen binding site and separate the binding sites of CO and O₂, preventing the CO poisoning. On the other hand, the Pd–Ag bimetallic system can lower the energy barriers of CO oxidation. In the CO–OO association pathway, the energy barrier for CO oxidation by the coadsorbed O₂ on the Pd–Ag bimetallic system is 0.45 eV, which is much lower than that (1.17 eV¹²) on the Pd monometallic system. In the direct O₂ dissociation pathway, the energy barrier for CO oxidation by the dissociated O atom on the Pd–Ag bimetallic system is 0.04 eV, which is also much lower than that (1.40 eV¹²) on the Pd monometallic system. These results indicate that the Pd–Ag bimetallic system tunes the catalytic activity by lowering the energy barriers of CO oxidation.

Palagin et al. showed that substitution of a Pd atom in the Pd₅ cluster by a single Ag atom to form Pd₄Ag₁ cluster leads to a potential improvement of the catalytic properties for the CO oxidation reaction,³⁵ which is in agreement with our result. Therefore, the Pd–Ag bimetallic system not only separates the binding sites of CO and O₂ but also facilitates CO oxidation by

reducing the reaction energy barriers. Experimentally, Bondarchuk et al. studied CO oxidation on Pd–Ag/SiO₂ bimetallic catalysts, and they also found that the activity of the bimetallic catalysts for CO oxidation increased compared with that of Pd/SiO₂ monometallic catalysts,³⁹ which is in agreement with our theoretical result. Pd–Ag bimetallic catalysts have also recently been reported to be catalytically active for various reactions.^{40,41}

4.3. Important Role of Metal–Metal Interface and Metal–Oxide Interface. It has been highlighted in previous studies that interfacial effects play an important role in catalytic reactions. Chen et al. studied interfacial effects in iron–nickel hydroxide–platinum nanoparticles and proposed that the OH groups at the Fe³⁺–OH–Pt interfaces react with adsorbed CO to produce CO₂.⁴² Rodriguez et al. found that the multifunctional combination of metal and oxide in the Cu–ceria and Au–ceria interfaces opens active reaction pathways for methanol synthesis.⁴³ Cargnello et al. found that the ceria–Pd interfacial sites greatly enhance CO oxidation reactivity on Pd/CeO₂ catalysts.¹⁸ Our results in this work indicate that both the metal–metal and metal–oxide interfaces play an important role in CO oxidation.

In section 3.2, the Pd–Ag interface is demonstrated to have bifunctional catalytic sites combining the advantages of the two metals and improving the CO oxidation activity. The Pd–Ag interface not only separates the binding sites of CO and O₂ but also reduces the energy barriers for CO oxidation as compared to the monometallic Pd system.¹² This improvement is attributed to a lower binding energy of O₂ at the Ag layer. Additionally, the adsorbed O₂ molecule can easily dissociate into two O atoms at the Pd–Ag interface, providing a second active reaction pathway for CO oxidation.

The metal–oxide interface also has a significant effect on CO oxidation. In section 3.2.3, we show that CO oxidation by M–vK mechanism at the Pd–CeO₂(111) interface is active in the Pd–Ag/CeO₂(111) system. Compared with the M–vK mechanism on clean CeO₂(111) surface studied by Chen et al.,⁴⁴ the energy barrier for CO oxidation by the M–vK mechanism on Pd–Ag/CeO₂(111) is lower (see Table 3). This difference is related to geometric distortions at the Pd–CeO₂

Table 3. Comparison of M–vK Mechanism on CeO₂(111)-Supported Pd–Ag Nanorod and Clean CeO₂(111) Surface

	energy barrier of CO oxidation (eV)	Ce–O bond length of active lattice O (Å)
CeO ₂ (111)-supported Pd–Ag nanorod	0.57	2.51
clean CeO ₂ (111)	0.61 ⁴⁴	2.37

interface, where the Pd metal layer strongly interacts with the CeO₂ support. As a result, the lattice oxygen atoms in the CeO₂ support adjacent to the Pd metal layer are pulled out by the Pd metal, leading to an elongation of Ce–O bonds to 2.51 Å at the Pd–CeO₂ interface as compared to 2.37 Å in the clean CeO₂(111) surface. Consistent with these results, Cargnello et al. reported a restructuring at the Pd–ceria interface when Pd metal particles were supported on the ceria surface.¹⁸ The increased Ce–O bond length is a good indication that the breaking of Ce–O bond is facilitated, and the activity of lattice oxygen is enhanced at the Pd–CeO₂ interface, promoting the CO oxidation. Therefore, the strong metal–support interaction at the Pd–CeO₂ interface facilitates the CO oxidation by M–vK mechanism.

Overall, our results suggest that the activity of metal/oxide catalysts can be improved by engineering a suitable bimetallic system which generates metal–metal and metal–oxide interfaces necessary for the binding and activation of CO and O₂.

5. CONCLUSIONS

A series of CeO₂(111)-supported Pd-based bimetallic nanorods (Pd–X, X = Ag, Au, Cu, Pt, Rh, Ru) were studied as CO oxidation catalysts using DFT calculations. Our results indicate that Pd–Ag/CeO₂ and Pd–Cu/CeO₂ are the two systems where the binding sites of CO and O₂ are distinct; that is, Pd sites prefer to bind CO, while Ag and Cu sites prefer to bind O₂. An analysis of the reaction mechanisms shows that Pd–Ag/CeO₂ is more effective for catalyzing CO oxidation than Pd–Cu/CeO₂ because both lattice O atoms of CeO₂ support and adsorbed O₂ molecules at Ag sites can oxidize CO with low energy barriers. Although the binding sites of CO and O₂ are separated in Pd–Cu/CeO₂, the lattice oxygen of the CeO₂ support cannot oxidize the adsorbed CO; only adsorbed O₂ at the Cu layer is active for CO oxidation, indicating that the CeO₂ support in the Pd–Cu/CeO₂ system has little direct effect on catalytic activity. Both the Pd–Ag and Pd–CeO₂ interfaces in the Pd–Ag/CeO₂ system were found to play important roles in CO oxidation. The Pd–Ag interface not only separates the binding sites of CO and O₂ but also facilitates CO oxidation. The strong metal–support interaction at the Pd–CeO₂ interface also facilitates CO oxidation by the M–vK mechanism. This study provides a theoretical guideline on the design of highly active metal/oxide catalysts for CO oxidation.

■ ASSOCIATED CONTENT

Supporting Information

The Supporting Information is available free of charge on the ACS Publications website at DOI: 10.1021/acs.jpcc.6b00253.

Surface coverage of CO and O₂ on all the bimetallic Pd–X/CeO₂ systems (Table S1) (PDF)

■ AUTHOR INFORMATION

Corresponding Authors

*E-mail zhenzhao@cup.edu.cn; Tel 86-10-89731586; Fax 86-10-69724721 (Z.Z.).

*E-mail henkelman@utexas.edu; Tel 5124714179; Fax 5124716835 (G.H.).

Notes

The authors declare no competing financial interest.

■ ACKNOWLEDGMENTS

The authors are grateful for financial support from Natural Science Foundation of China (21503273, 21477164, 21376261, 21173270, and 21177160), Beijing Natural Science Foundation (2142027), China Scholarship Council (201406440013), Science Foundation of China University of Petroleum-Beijing (No.ZX20150025). Computing time in the National Super Computing Center in Jinan is acknowledged. The work in Austin was supported by the Department of Energy (DE-FG02-13ER16428), the Welch Foundation (F-1841), and the Texas Advanced Computing Center.

■ REFERENCES

- (1) Song, W.; Hensen, E. J. M. A Computational DFT Study of CO Oxidation on a Au Nanorod Supported on CeO₂(110): On the Role of the Support Termination. *Catal. Sci. Technol.* **2013**, *3*, 3020–3029.
- (2) Kim, H. Y.; Henkelman, G. CO Oxidation at the Interface of Au Nanoclusters and the Stepped-CeO₂(111) Surface by the Mars-van Krevelen Mechanism. *J. Phys. Chem. Lett.* **2013**, *4*, 216–221.
- (3) Sun, C.; Li, H.; Chen, L. Nanostructured Ceria-Based Materials: Synthesis, Properties, and Application. *Energy Environ. Sci.* **2012**, *5*, 8475–8505.
- (4) Zhang, C. J.; Michaelides, A.; Jenkins, S. J. Theory of Gold on Ceria. *Phys. Chem. Chem. Phys.* **2010**, *13*, 22–33.
- (5) Zhu, W. J.; Zhang, J.; Gong, X. Q.; Lu, G. A Density Functional Theory Study of Small Au Nanoparticles at CeO₂ Surfaces. *Catal. Today* **2011**, *165*, 19–24.
- (6) Wang, R.; He, H.; Liu, L.; Dai, H.; Zhao, Z. Shape-Dependent Catalytic Activity of Palladium Nanocrystals for the Oxidation of Carbon Monoxide. *Catal. Sci. Technol.* **2012**, *2*, 575–580.
- (7) Jin, M.; Park, J.; Shon, J. K.; Kim, J. H.; Li, Z.; Park, Y.; Kim, J. M. Low Temperature CO Oxidation over Pd Catalysts Supported on Highly Ordered Mesoporous Metal Oxides. *Catal. Today* **2012**, *185*, 183–190.
- (8) Wang, J.; Chen, H.; Hu, Z.; Yao, M.; Li, Y. A Review on the Pd-Based Three-Way Catalyst. *Catal. Rev.: Sci. Eng.* **2015**, *57*, 79–114.
- (9) Shen, M.; Yang, M.; Wang, J.; Wen, J.; Zhao, M.; Wang, W. Pd/Support Interface-Promoted Pd-Ce_{0.7}Zr_{0.3}O₂-Al₂O₃ Automobile Three-Way Catalysts: Studying the Dynamic Oxygen Storage Capacity and CO, C₃H₈, and NO Conversion. *J. Phys. Chem. C* **2009**, *113*, 3212–3221.
- (10) Zhu, H.; Qin, Z.; Shan, W.; Shen, W.; Wang, J. Low-Temperature Oxidation of CO over Pd/CeO₂-TiO₂ Catalysts with Different Pretreatment. *J. Catal.* **2005**, *233*, 41–50.
- (11) Liu, J.; Liu, B.; Fang, Y.; Zhao, Z.; Wei, Y.; Gong, X.-Q.; Xu, C.; Duan, A.; Jiang, G. Preparation, Characterization and Origin of Highly Active and Thermally Stable Pd-Ce_{0.8}Zr_{0.2}O₂ Catalysts via Sol-Evaporation Induced Self-Assembly Method. *Environ. Sci. Technol.* **2014**, *48*, 12403–12410.
- (12) Liu, B.; Liu, J.; Li, T.; Zhao, Z.; Gong, X.-Q.; Chen, Y.; Duan, A.; Jiang, G.; Wei, Y. Interfacial Effects of CeO₂-Supported Pd Nanorod in Catalytic CO Oxidation: A Theoretical Study. *J. Phys. Chem. C* **2015**, *119*, 12923–12934.
- (13) Somorjai, G. A.; Li, Y. *Introduction to Surface Chemistry and Catalysis*; Wiley: New York, 2010.
- (14) Mu, R.; Fu, Q.; Xu, H.; Zhang, H.; Huang, Y.; Jiang, Z.; Zhang, S.; Tan, D.; Bao, X. Synergetic Effect of Surface and Subsurface Ni

Species at Pt-Ni Bimetallic Catalysts for CO Oxidation. *J. Am. Chem. Soc.* **2011**, *133*, 1978–1986.

(15) Tao, F. Synthesis, Catalysis, Surface Chemistry and Structure of Bimetallic Nanocatalysts. *Chem. Soc. Rev.* **2012**, *41*, 7977–7979.

(16) Green, I. X.; Tang, W.; Neurock, M.; Yates, J. T. Insights into Catalytic Oxidation at the Au/TiO₂ Dual Perimeter Sites. *Acc. Chem. Res.* **2014**, *47*, 805–815.

(17) Kim, H. Y.; Henkelman, G. CO Oxidation at the Interface between Doped CeO₂ and Supported Au Nanoclusters. *J. Phys. Chem. Lett.* **2012**, *3*, 2194–2199.

(18) Cargnello, M.; Donan-Nguyen, V. V. T.; Gordon, T. R.; Diaz, R. E.; Stach, E. A.; Gorte, R. J.; Fornasiero, P.; Murray, C. B. Control of Metal Nanocrystal Size Reveals Metal-Support Interface Role for Ceria Catalysts. *Science* **2013**, *341*, 771–773.

(19) Zhou, Z.; Kooi, S.; Flytzani-Stephanopoulos, M.; Saltsburg, H. The Role of the Interface in CO Oxidation on Au/CeO₂ Multilayer Nanotowers. *Adv. Funct. Mater.* **2008**, *18*, 2801–2807.

(20) Park, J. B.; Graciani, J.; Evans, J.; Stacchiola, D.; Senanayake, S. D.; Barrio, L.; Liu, P.; Sanz, J. F.; Hrbek, J.; Rodriguez, J. A. Gold, Copper, and Platinum Nanoparticles Dispersed on CeO_x/TiO₂(110) Surfaces: High Water-Gas Shift Activity and the Nature of the Mixed-Metal Oxide at the Nanometer Lever. *J. Am. Chem. Soc.* **2010**, *132*, 356–363.

(21) Bruix, A.; Rodriguez, J. A.; Ramirez, P. J.; Senanayake, S. D.; Evans, J.; Park, J. B.; Stacchiola, D.; Liu, P.; Hrbek, J.; Illas, F. A New Type of Strong Metal-Support Interaction and the Production of H₂ through the Transformation of Water on Pt/CeO₂(111) and Pt/CeO_x/TiO₂(110) Catalysts. *J. Am. Chem. Soc.* **2012**, *134*, 8968–8974.

(22) Aranifard, S.; Ammal, S. C.; Heyden, A. On the Importance of Metal–Oxide Interface Sites for the Water–Gas Shift Reaction over Pt/CeO₂ Catalysts. *J. Catal.* **2014**, *309*, 314–324.

(23) Schalow, T.; Laurin, M.; Brandt, B.; Schauermann, S.; Guimond, S.; Kühlenbeck, H.; Starr, D. E.; Shaikhutdinov, S. K.; Libuda, J.; Freund, H. J. Oxygen Storage at the Metal/Oxide Interface of Catalyst Nanoparticles. *Angew. Chem., Int. Ed.* **2005**, *44*, 7601–7605.

(24) Kresse, G.; Furthmüller, J. Efficient Iterative Schemes for Ab Initio Total-Energy Calculations Using a Plane-Wave Basis Set. *Phys. Rev. B: Condens. Matter Mater. Phys.* **1996**, *54*, 11169–11186.

(25) Kresse, G.; Furthmüller, J. Efficiency of Ab-Initio Total Energy Calculation for Metals and Semiconductors Using a Plane-Wave Basis Set. *Comput. Mater. Sci.* **1996**, *6*, 15–50.

(26) Dudarev, S. L.; Botton, G. A.; Savrasov, S. Y.; Humphreys, C. J.; Sutton, A. P. Electron-Energy-Loss Spectra and the Structural Stability of Nickel Oxide: An LSDA+U Study. *Phys. Rev. B: Condens. Matter Mater. Phys.* **1998**, *57*, 1505–1509.

(27) Nolan, M.; Parker, S. C.; Watson, G. W. CeO₂ Catalysed Conversion of CO, NO₂ and NO from First Principles Energetics. *Phys. Chem. Chem. Phys.* **2006**, *8*, 216–218.

(28) Yang, Z.; Luo, G.; Lu, Z.; Hermansson, K. Oxygen Vacancy Formation Energy in Pd-Doped Ceria: A DFT+U Study. *J. Chem. Phys.* **2007**, *127*, 074704.

(29) Blöchl, P. E. Projector Augmented-Wave Method. *Phys. Rev. B: Condens. Matter Mater. Phys.* **1994**, *50*, 17953–17979.

(30) Perdew, J. P.; Burke, K.; Ernzerhof, M. Generalized Gradient Approximation Made Simple. *Phys. Rev. Lett.* **1996**, *77*, 3865–3868.

(31) Henkelman, G.; Jonsson, H. Improved Tangent Estimate in the Nudged Elastic Band Method for Finding Minimum Energy Paths and Saddle Points. *J. Chem. Phys.* **2000**, *113*, 9978–9985.

(32) Henkelman, G.; Uberuaga, B. P.; Jonsson, H. A Climbing Image Nudged Elastic Band Method for Finding Saddle Points and Minimum Energy Paths. *J. Chem. Phys.* **2000**, *113*, 9901–9904.

(33) Nolan, M.; Grigoleit, S.; Sayle, D. C.; Parker, S. C.; Watson, G. W. Density Functional Theory Studies of the Structure and Electronic Structure of Pure and Defective Low Index Surfaces of Ceria. *Surf. Sci.* **2005**, *576*, 217–229.

(34) Cen, W.; Liu, Y.; Wu, Z.; Wang, H.; Weng, X. A Theoretic Insight into the Catalytic Activity Promotion of CeO₂ Surfaces by Mn Doping. *Phys. Chem. Chem. Phys.* **2012**, *14*, 5769–5777.

(35) Palagin, D.; Doye, J. P. K. CO Oxidation Catalysed by Pd-Based Bimetallic Nanoalloys. *Phys. Chem. Chem. Phys.* **2015**, *17*, 28010–28021.

(36) Zhang, L.; Kim, H. Y.; Henkelman, G. CO Oxidation at the Au-Cu Interface of Bimetallic Nanoclusters Supported on CeO₂(111). *J. Phys. Chem. Lett.* **2013**, *4*, 2943–2947.

(37) Vayssilov, G. N.; Lykhach, Y.; Migani, A.; Staudt, T.; Petrova, G. P.; Tsud, N.; Skala, T.; Bruix, A.; Illas, F.; Prince, K. C.; et al. Support Nanostructure Boosts Oxygen Transfer to Catalytically Active Platinum Nanoparticles. *Nat. Mater.* **2011**, *10*, 310–315.

(38) Kim, H. Y.; Lee, H. M.; Henkelman, G. CO Oxidation Mechanism on CeO₂-Supported Au Nanoparticles. *J. Am. Chem. Soc.* **2012**, *134*, 1560–1570.

(39) Bondarchuk, I. S.; Mamontov, G. V. Role of PdAg Interface in Pd–Ag/SiO₂ Bimetallic Catalysts in Low-Temperature Oxidation of Carbon Monoxide. *Kinet. Catal.* **2015**, *56*, 379–385.

(40) Yin, Z.; Zhang, Y.; Chen, K.; Li, J.; Li, W.; Tang, P.; Zhao, H.; Zhu, Q.; Bao, X.; Ma, D. Monodispersed Bimetallic PdAg Nanoparticles with Twinned Structures: Formation and Enhancement for the Methanol Oxidation. *Sci. Rep.* **2014**, *4*, 4288.

(41) Cui, Z.; Yang, M.; DiSalvo, F. J. Mesoporous Ti_{0.5}Cr_{0.5}N Supported PdAg Nanoalloy as Highly Active and Stable Catalysts for the Electro-Oxidation of Formic Acid and Methanol. *ACS Nano* **2014**, *8*, 6106–6113.

(42) Chen, G.; Zhao, Y.; Fu, G.; Duchesne, P. N.; Gu, L.; Zheng, Y.; Weng, X.; Chen, M.; Zhang, P.; Pao, C.-W.; et al. Interfacial Effects in Iron-Nickel Hydroxide-Platinum Nanoparticles Enhance Catalytic Oxidation. *Science* **2014**, *344*, 495–499.

(43) Rodriguez, J. A.; Liu, P.; Stacchiola, D. J.; Senanayake, S. D.; White, M. G.; Chen, J. G. Hydrogenation of CO₂ to Methanol: Importance of Metal–Oxide and Metal–Carbide Interfaces in the Activation of CO₂. *ACS Catal.* **2015**, *5*, 6696–6706.

(44) Chen, F.; Liu, D.; Zhang, J.; Hu, P.; Gong, X.-Q.; Lu, G. A DFT +U Study of the Lattice Oxygen Reactivity toward Direct CO Oxidation on the CeO₂(111) and (110) Surfaces. *Phys. Chem. Chem. Phys.* **2012**, *14*, 16573–16580.